Marginal-Zone B-Cells of Nonobese Diabetic Mice Expand With Diabetes Onset, Invade the Pancreatic Lymph Nodes, and Present Autoantigen to Diabetogenic T-Cells

Eliana Mariño, Marcel Batten, Joanna Groom, Stacey Walters, David Liuwantara, Fabienne Mackay, and Shane T. Grey

OBJECTIVE—B-cells are important for disease pathogenesis in the nonobese diabetic (NOD) mouse model of type 1 diabetes. Recent studies demonstrate that marginal-zone B-cells (MZBs), which connect innate with adaptive immune responses, are increased in NOD mice. However, beyond this, the contribution of different B-cell subsets to diabetes pathogenesis is poorly understood.

RESEARCH DESIGN AND METHODS—To better understand the role of different B-cell subsets in the etiology of type 1 diabetes, we have examined the MZB compartment in NOD mice, with respect to their number, distribution, and function.

RESULTS—We demonstrate that splenic MZB numbers in female NOD mice undergo a marked, approximately threefold expansion between ~12 and 16 weeks of age, coincident with the onset of frank diabetes. Functionally, NOD MZBs are hyperresponsive to toll-like receptor 9 ligation and CD40 ligation, as well as sphingosine-1-phosphate–dependent chemotactic cues, suggesting an increased sensitivity to selective innate- and activation-induced stimuli. Intriguingly, at 16 weeks of age, ~80% of female NOD mice present with MZB-like cells in the pancreatic lymph node (PLN). These MZB-like cells express major histocompatibility complex class II and high levels of CD80 and CD86, and their presence in the PLN is associated with an increased frequency of activated $V\beta4^+$ $CD4^+$ T-cells. Significantly, we demonstrate that purified MZBs are able to present the autoantigen insulin to diabetogenic T-cells.

CONCLUSIONS—These data are consistent with MZBs contributing to the pathogenesis of type 1 diabetes as antigen-presenting cells. By integrating innate-derived inflammatory signals with the activation of autoreactive T-cells, MZBs may help to direct T-cell responses against β-cell self-constituents. ***Diabetes*** **57:395–404, 2008**

From the Immunology and Inflammation Program, Garvan Institute of Medical Research, New South Wales, Australia.

Address correspondence and reprint requests to Shane T. Grey, PhD, Senior Research Fellow, Gene Therapy and Autoimmunity Group, Arthritis and Inflammation Program, Garvan Institute of Medical Research, 384 Victoria St., Darlinghurst, N5W 2010, Australia. E-mail: s.grey@garvan.org.au.

Received for publication 29 April 2007 and accepted in revised form 12 November 2007.

Published ahead of print at http://diabetes.diabetesjournals.org on 19 November 2007. DOI: 10.2337/db07-0589.

APC, antigen-presenting cell; BAFF, B-cell activator from the tumor necrosis factor family; BrdU, 5-bromo-2-deoxyuridine; FACS, fluorescence-activated cell sorter; FoB, follicular B-cell; GAPDH, glyceraldehyde 3-phosphate dehydrogenase; ILN, inguinal lymph node; MHC, major histocompatibility complex; MLN, mesenteric lymph node; MZB, marginal-zone B-cell; NF, nuclear factor; PLN, pancreatic lymph node; S1P, sphingosine-1-phosphate; TLR, toll-like receptor.

Splenic B-cells play a necessary role in diabetes pathogenesis in the nonobese diabetic (NOD) mouse model of type 1 diabetes (1–3) by secreting an antibody that is required for diabetes initiation (4) but also by presenting self-antigens including insulin to autoreactive T-cells (5–7). B-cell development proceeds in the spleen to give rise to two mature subsets: follicular B-cells (FoBs) and marginal-zone B-cells (MZBs) (8,9). There is emerging evidence from the NOD model that MZBs may be an important B-cell subset in diabetes pathogenesis (1). NOD mice exhibit significantly increased numbers of MZBs compared with non–autoimmune-prone strains (10,11). Moreover, elimination of a $CD21^+$ $CD1d^{hi}$ MZB-like population by way of a depleting anti-CD21/35 (CR1/2 [complement receptor 1/2]) monoclonal abs reduced disease incidence in an experimental model of diabetes (12). Given the caveat that this study did not identify the depleted cells as MZBs, and that blockade of CD21/35 may have diverse effects on multiple cell populations, this was still an intriguing result potentially linking MZBs to type 1 diabetes development. Linkage of the expanded MZB phenotype in NOD mice to a number of genetic loci (10), including one major region on chromosome 4 colocalizing with the diabetes susceptibility locus *Idd*9/11, was also suggestive of a role of MZBs in type 1 diabetes pathogenesis.

MZBs are located within the marginal sinus of the spleen (9,13) and exhibit an activated effector phenotype, as indicated by their ability to generate rapid antibody responses to antigens and blood-borne pathogens (14–17). In addition, MZBs are able to act as efficient antigen-presenting cells (APCs), providing cognate help to naïve $CD4^+$ T-cells (18) and, in this way, may connect innate with adaptive immune responses (9,19). Significantly, emerging studies from the B-cell activator from the tumor necrosis factor family (BAFF) transgenic and New Zealand black × New Zealand white (NZB/W) F1 mice indicate that MZBs may also be involved in the development of autoimmune conditions. BAFF transgenic and NZB/W F1 mice exhibit an increased frequency of splenic MZBs (20,21), harbor high titers of circulating antibodies directed against self-constituents, and develop autoimmune conditions reminiscent of lupus and sialadenitis (22,23).

The ability of MZBs to respond to innate signals, generate antigen-specific antibody responses, as well as present antigen to naïve T-cells lends support to their potential as players in the development of autoimmunity (1,24). De-

spite studies (10–12) indicating their expanded nature, the role of MZBs in diabetes pathogenesis in the NOD model is unknown. To better understand their role in the etiology of type 1 diabetes, we have examined the MZB compartment in NOD mice with respect to their number, distribution, and function. We provide novel evidence that MZBs, by virtue of their capacity to integrate innate-derived inflammatory signals with the presentation of autoantigens, may help to direct T-cell responses against β-cells.

RESEARCH DESIGN AND METHODS

Mice. C57BL/6, BALB/c, and CBA mice were obtained from the Animal Resource Center (Perth, Western Australia, Australia). NOD/Lt (NOD) mice were obtained from the Walter and Elisa Hall Institute (Melbourne, Australia). Mice were monitored for diabetes twice weekly from 10 weeks of age onwards, as described (25). The incidence of diabetes in NOD mice in our facility is ~80% by 40 weeks of age. All experimental procedures were conducted using 6- to 10-week-old mice, unless otherwise specified. All animal experiments were performed with the approval of the St. Vincent's Campus Animal Experimentation Committee.

Flow cytometry. Lymphocytes were isolated from spleen, peripheral lymph nodes (PLNs), and pancreata of various strains of mice using standard techniques. Primary biotin–fluorescein isothiocyanate–, phycoethrin-, PerCP-, and APC-labeled monoclonal rat antibodies against mouse cell-surface antigens B220/CD45R (RA-6B2), CD4 (GK1.5), CD8a (53-6-7), IgM (11/41), CD21/CD35 (7G6), CD23/Fc RII (B3B4), CD1d/CD1.1/Ly-3B (1B1), CD9 (KMC8), CD44 (Pgp-1, Ly-24) (IM7), Vβ4 T-cell receptor (KT4), I-A^K (AB^K) (10-3.6), CD86 (B7-2) (GL1), CD80 (B7-1) (16-10A1), as well as secondary reagents, were purchased from BD Biosciences (San Jose, CA). Flow cytometric analysis was conducted on a FACScalibur flow cytometer (BD Biosciences). Splenic B-cell subpopulations were identified based on the expression pattern of IgM, B220, CD21, and CD23, as described by Loder et al. (8). Thus, FoBs are defined as $CD23^{hi}$, IgM^{+}, and $CD21^{low}$ cells; MZBs and MZB-like cells are defined as $CD23^{low}$, IgM^{hi} $CD21^{hi}$, $CD1d^{hi}$, and $CD9^{hi}$ cells.

Histology. Freshly isolated splenic tissue was snap frozen and later analyzed by immunohistochemistry using anti-mouse CD1d-biotin (BD Biosciences) and rat anti-mouse Moma-1 (Serotec/Australia Laboratory Services). Primary antibody labeling was revealed with horseradish peroxidase–linked anti-rat

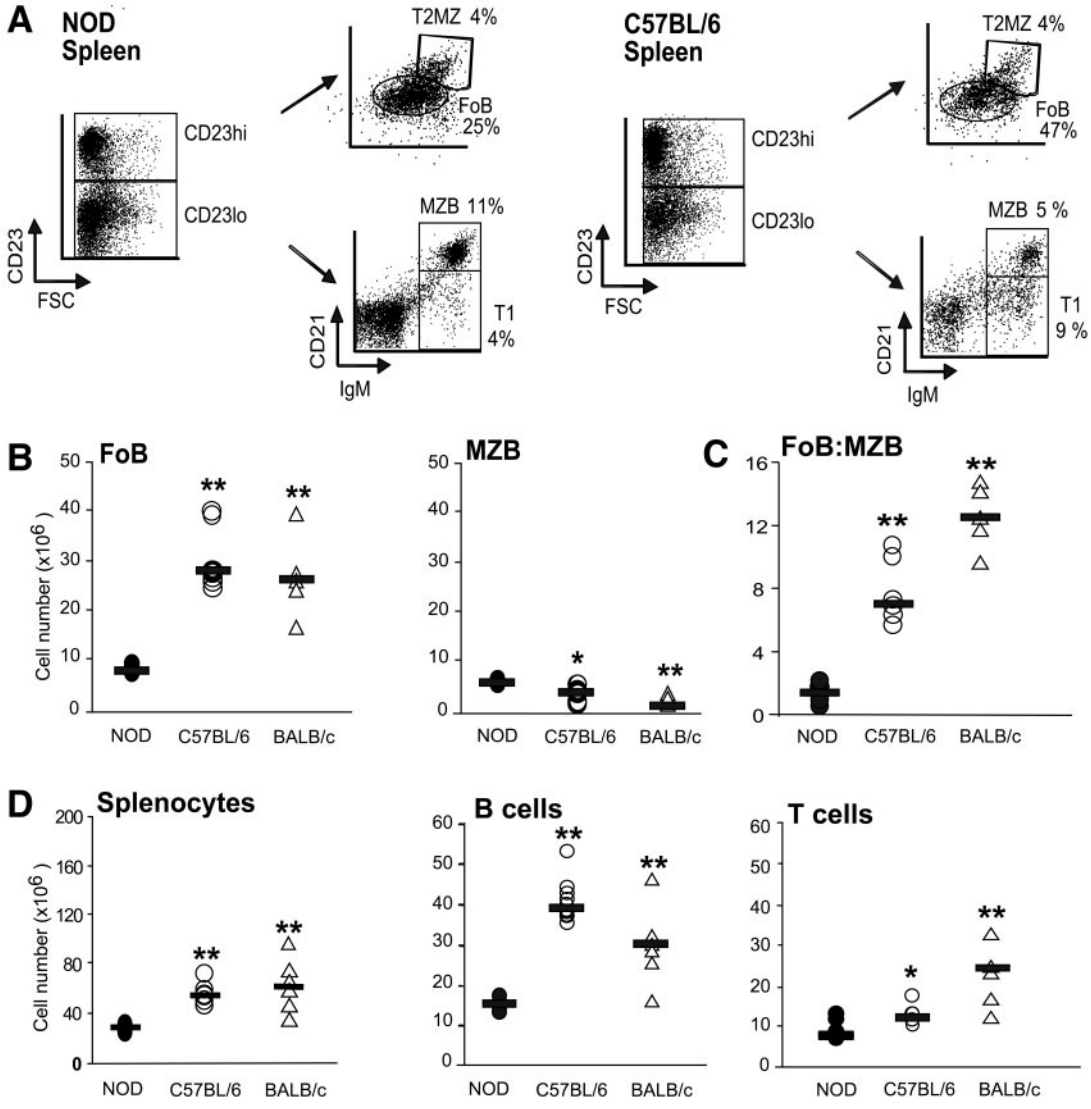

FIG. 1. NOD mice have an expanded number of MZBs. *A*: Representative FACS plots illustrating gating strategy to enumerate splenic B-cell subsets in 5-week-old female NOD and C57BL/6 mice. Numbers represent percentage of total lymphocytes. T1, transitional T1 cell; T2MZ, transitional T2MZ cell. Results from one of at least six independent experiments are shown. *B*: Absolute numbers of FoBs and MZBs. Results represent values from individual mice ($n \geq 5$ per group), bar represents median value. *C*: Ratio of FoBs to MZBs in 5-week-old female NOD, C57BL/6, and BALB/c mice, calculated from absolute numbers presented in (*B*). Results represent values from individual mice ($n \geq 5$ per group), bar represents median value. *D*: Absolute numbers of splenocytes, B-cells, and T-cells in 5-week-old female NOD, C57BL/6, and BALB/c mice. Results represent values from individual mice ($n \geq 5$ per group), bar represents median value. All results are from 5-week-old female mice. ●, NOD mice; ○, C57BL/6; and △, BALB/c mice. *P* values represent comparison between NOD and age-matched control strain. *$P < 0.05$; **$P < 0.01$; ***$P < 0.001$.

IgG and alkaline phosphatase–linked streptavidin. Chromogenic substrate reagents diaminobenzidine (Sigma) and NBT/BCIP (Sigma) were used to develop horseradish peroxidase and alkaline phosphatase, respectively.

Sphingosine-1-phosphate receptor expression. Expression of the sphingosine-1-phosphate (S1P) receptors S1P1 and SIP3 on fluorescence-activated cell sorter (FACS)-purified FoB and MZBs was determined by quantitative real-time PCR as described (26). Primers for S1P1, S1P3, and glyceraldehyde 3-phosphate dehydrogenase (GAPDH) are listed as follows: S1P1 forward 5′GCGCTCAGAGACTTCGTCTT3′, reverse 5′ACCAGCT CACTCGCAAAGTT3′; S1P3 forward 5′CCTTGCAGAACGAGAGCCTA3′, reverse 5′TTCCCGGAGAGTGTCATTTC3′; and GAPDH forward 5′CTCAT GACCACAGTCCATGC3′. All values were normalized to GAPDH mRNA levels.

Chemotaxis assays. Responses to S1P were determined essentially as described (27). Briefly, 5×10^5 splenocytes were seeded in the upper chamber of transwell plates with a 3-μm filter (Corning Costar, Lindfield, NSW, Australia). Transmigration of B-cell subpopulations in response to increasing concentrations of recombinant S1P (Sigma) (0.1–10 nmol/l) was assessed after 3 h by phenotypic analysis (FACS) of cell populations in the lower chamber.

In vitro B-cell stimulation assays. Splenic B-cells were purified from 5-week-old NOD mice using a MACS Pan-B-cell isolation kit (Miltenyi Biotec, Sydney, Australia). FoB and MZB populations were sorted to 90% purity on a FACSAria cell sorter (BD Biosciences) based upon the expression of IgM, B220, CD21, and CD23. For in vitro stimulation assays, cells were seeded at 1×10^5 per well into round-bottom microtitre plates in 100 μl medium (RPMI-1650; Life Technologies/Invitrogen; 10% heat-inactivated FCS and 1:100 penicillin/streptomycin; Gibco Life Technologies; and 50 μmol/l 2-mercaptoethanol; Merck) and cultured in triplicate with either the F(ab)2 fragment of goat anti-murine IgM (μ-chain specific, 20 μg/ml; Jackson Immunoresearch), interleukin-4 (100 ng/ml; Gibco/Invitrogen), anti-mouse CD40 (HM40-3) (1 μg/ml; BD Biosciences), lipopolysaccharide (500 ng/ml; Gibco/Invitrogen), or bacterial DNA (CpG dinucleotide) (3 μg/ml; Gibco/Invitrogen) for 48 h. Cells were pulsed for the last 24 h with ^{3}[H]-thymidine (1 μCi/well; Amersham Biosciences), harvested, and then assayed for ^{3}[H]-thymidine incorporation (cpm).

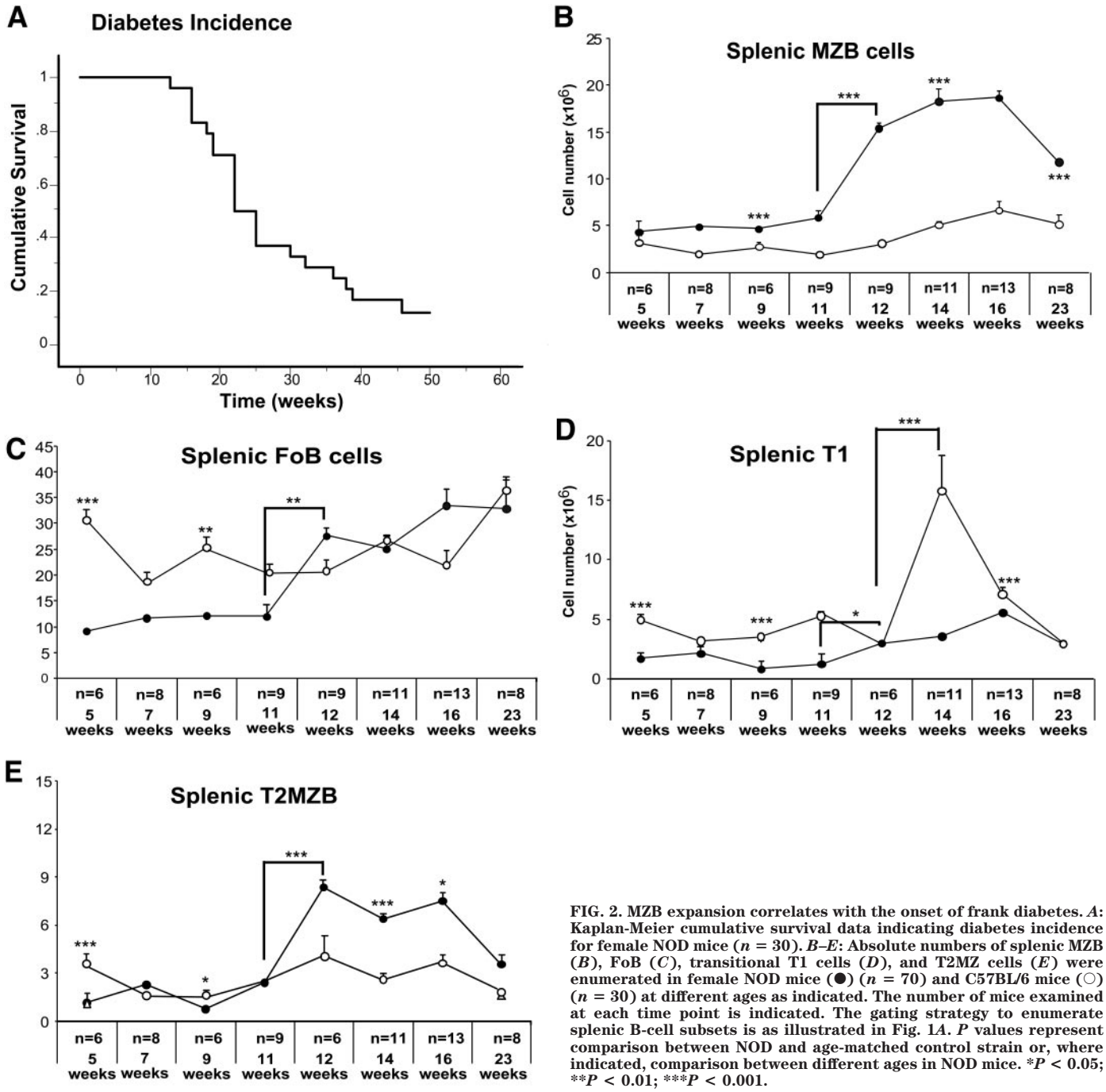

FIG. 2. MZB expansion correlates with the onset of frank diabetes. *A*: Kaplan-Meier cumulative survival data indicating diabetes incidence for female NOD mice ($n = 30$). *B–E*: Absolute numbers of splenic MZB (*B*), FoB (*C*), transitional T1 cells (*D*), and T2MZ cells (*E*) were enumerated in female NOD mice (●) ($n = 70$) and C57BL/6 mice (○) ($n = 30$) at different ages as indicated. The number of mice examined at each time point is indicated. The gating strategy to enumerate splenic B-cell subsets is as illustrated in Fig. 1*A*. *P* values represent comparison between NOD and age-matched control strain or, where indicated, comparison between different ages in NOD mice. *$P < 0.05$; **$P < 0.01$; ***$P < 0.001$.

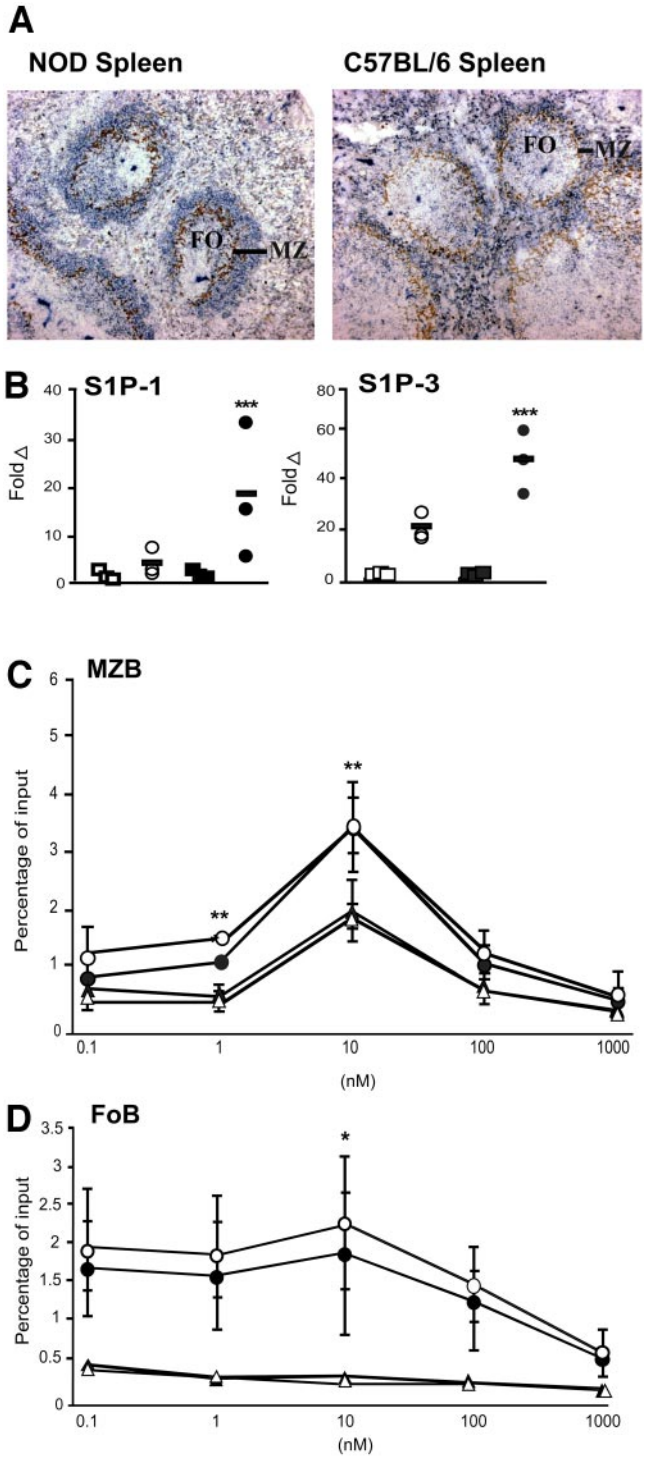

FIG. 3. Dysregulated S1P signaling in NOD mice. *A*: Altered splenic architecture of NOD mice. Representative histological section illustrating splenic architecture from a NOD and C57BL/6 mice. Identification of metallophilic macrophages (MOMA-1; brown) and MZBs (CD1d; blue). FO, follicular area; MZ, marginal zone. *B*: Semiquantitative RT-PCR analysis of S1P1 and S1P3 mRNA expression in FACS-purified FoBs (squares) or MZBs (circles) isolated from NOD (filled symbols) or C57BL/6 (open symbols) mice. Results represent fold change in S1P receptor expression relative to GAPDH for individual mice ($n = 3$ per group), bar represents median value. *C*: Chemotactic response of FACS-purified NOD (circles) and C57BL/6 (triangles) MZBs to increasing concentrations of S1P with (filled symbols) or without (open symbols) FTY720 pretreatment. Results represent meansa ± SE of one representative experiment ($n = 3$ mice per group) of four independent experiments conducted. *D*: As for (*C*), except FoB migration is shown. *P* value indicates comparison between NOD and C57BL/6 mice. *$P < 0.05$; **$P < 0.01$; ***$P < 0.001$. (A high-quality digital representation of this figure can be found at http://dx.doi.org/10.2337/db07-0589.)

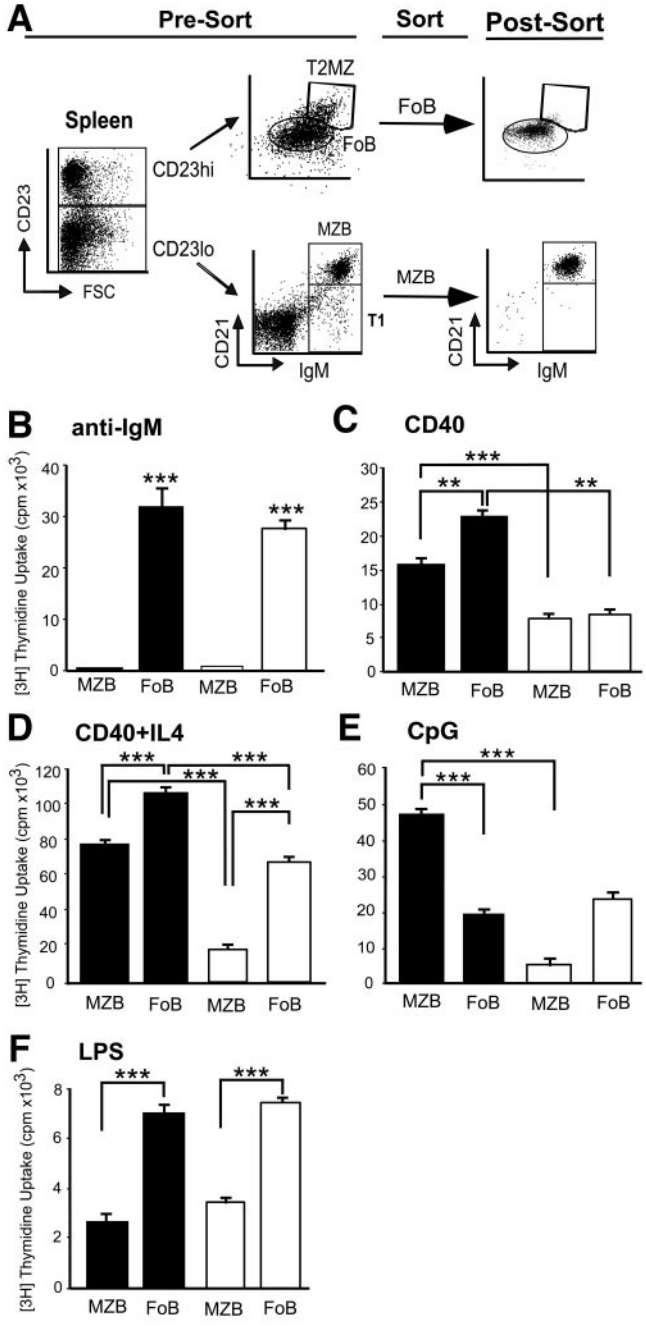

FIG. 4. NOD MZBs are selectively hyperresponsive to TLR9 ligation and CD40 ligation. *A*: Representative FACS plot demonstrating sorting protocol to achieve pure MZB and FoB populations. *B–F*: Proliferative responses (cpm) of purified MZBs or FoBs stimulated with anti-mμ (20 μg/ml) (*B*), CD40 (1 μg/ml) (*C*), CD40 (1 μg/ml) plus interleukin-4 (100 ng/ml) (*D*), CpG dinucleotide (3 μg/ml) (*E*), or LPS (500 ng/ml)-stimulated B-cells (*F*). Background proliferation was 500 cpm. Data represents mean (cpm) ± SE of triplicate samples from one of six independent experiments conducted. *$P < 0.05$; **$P < 0.01$; ***$P < 0.001$.

Antigen presentation assays. For in vivo T-cell priming, female NOD mice were immunized on the hind flank with 50 μg of the insulin peptide B9:23 SHLVEALYLVCGERG (Mimotopes, Clayton, Australia) in Freunds' complete adjuvant. Seven days later, T-cells from the local lymph nodes were isolated by a MACS Pan-T-cell isolation kit (Miltenyi Biotec). Splenic B-cells, FoBs, or MZBs were obtained as above. For the assay, 2.5 × 105 T-cells were cultured with either 2.5 × 105 total B-cells, MZBs, or FoBs primed with either 200 μg B9:23 peptide or 200 μg purified porcine insulin (I5523; Sigma). Cultures were pulsed at 72 h for the last 16 h with ^{3}[H]-thymidine (1μCi/well; Amersham Biosciences), harvested, and then assayed for ^{3}[H]-thymidine incorporation

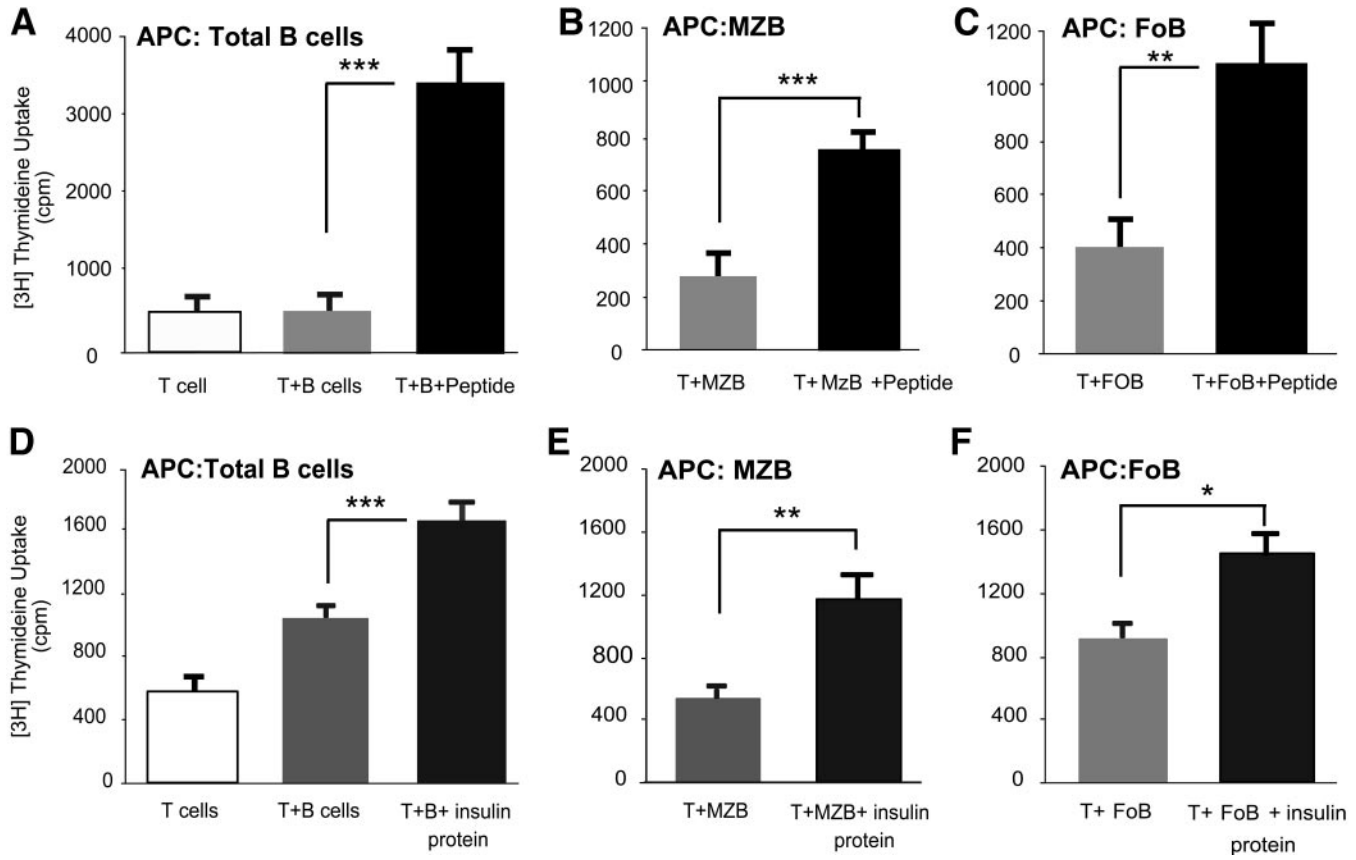

FIG. 5. NOD MZB present autoantigen to diabetogenic T-cells. T-cell proliferation induced by unfractionated splenic B-cells (*A* and *D*), sorted MZBs (*B* and *E*), or sorted FoBs (*C* and *F*). T-cells were cultured for 86 h with either insulin peptide B9:23-pulsed (200 μg/well) B-cell populations (*A–C*) or intact insulin-pulsed (200 μg/well) B-cell populations (*D–F*). Cultures were pulsed for the last 16 h with ^{3}[H]-thymidine. Data represents mean (cpm) ± SE of triplicate samples from a representative experiment of five independent experiments conducted. In each case, *P* value indicates comparison between T-cells plus APCs and T-cells plus antigen-pulsed APCs. **P* < 0.05; ***P* < 0.01; ****P* < 0.001.

(cpm). Preliminary experiments established this to be the optimal protocol to assess APC activity.

5-Bromo-2-deoxyuridine proliferation assays. To determine whether the increase in MZB-like cells in the PLN related to migration or proliferation locally, 6- and 16-week-old female NOD mice were pulsed with 5-bromo-2-deoxyuridine (BrdU) (2 mg/kg) for 3 consecutive days and assessed for BrdU incorporation on day 4 by a FACScalibur flow cytometer (BD Biosciences). B-cell subpopulations were identified by FACS, as described above.

Statistics. Statistical significance was determined by calculating *P* values using a Mann-Whitney and *t* test on Instat software (GraphPad Softward, San Diego, CA).

RESULTS

Kinetics of MZB expansion in NOD mice. NOD mice have a phenotypically altered B-cell compartment favoring an increased frequency of MZBs (10,11). In young NOD mice, this relates to a ~70% decrease in the absolute numbers of FoBs ($n \geq 5$) ($P < 0.01$), and a small, but significant, increase in MZB numbers of over that seen in C57BL/6 and BALB/c mice (increased ~1.4-fold, $P < 0.05$, $n \geq 5$ and ~2-fold, $P < 0.01$, $n \geq 5$, respectively) (Fig. 1*A–C*). The marked decrease in FoB numbers contributes to marked lymphopenia, evidenced by the reduced number of total splenocytes in female NOD mice (Fig. 1*D*). The relative decrease in FoB numbers combined with the minor increase in MZB numbers manifested as a marked alteration in the FoB-to-MZB ratio in NOD mice; this ratio was decreased from ~10:1 (FoB:MZB) in C57BL/6 and BALB/c mice to ~2:1 in NOD mice ($n \geq 5$) ($P < 0.01$) (Fig. 1*C*).

An additional unusual feature of the NOD MZB population is that their numbers increase in parallel with insulitis (11). However, the relationship between their expansion and the onset of overt diabetes, which occurs from ~13 weeks of age and onwards in NOD mice, has not been investigated. Accordingly, we conducted a longitudinal study of splenic MZB numbers in a cohort of female NOD mice ($n = 70$) from 5 to 23 weeks of age to determine how the expansion in MZB numbers correlated with diabetes development. In our control cohort of female NOD mice ($n = 30$), frank diabetes manifested at ~13 weeks of age, reaching an incidence of ~70% by 30 weeks of age (Fig. 2*A*). Analysis of MZB numbers revealed that the absolute number of MZBs dramatically increased approximately threefold ($n \geq 6$) ($P < 0.001$) from a steady state of ~5×10^6 at 11 weeks of age to ~15×10^6 at 12 weeks of age (Fig. 2*B*). In contrast, no changes were observed in MZBs in C57BL/6 mice over this same period. The MZB expansion was accompanied by an approximately threefold increase in FoB numbers ($n \geq 6$) ($P < 0.01$) from ~10×10^6 at 11 weeks of age to ~27×10^6 at 12 weeks of age (Fig. 2*C*). Thus, the lymphopenic state of young NOD mice (28) is due to a marked reduction in the numbers of FoBs, which corrects at ~12 weeks of age due to an expansion of both MZBs and FoBs, just before the occurrence of frank diabetes. The change in MZB number at this time may relate to an underlying alteration in the dynamic-controlling B-cell development, as there was a parallel increase in the absolute numbers of T2MZ transitional B-cell precursors in the spleen. Thus, T2MZ increased approximately

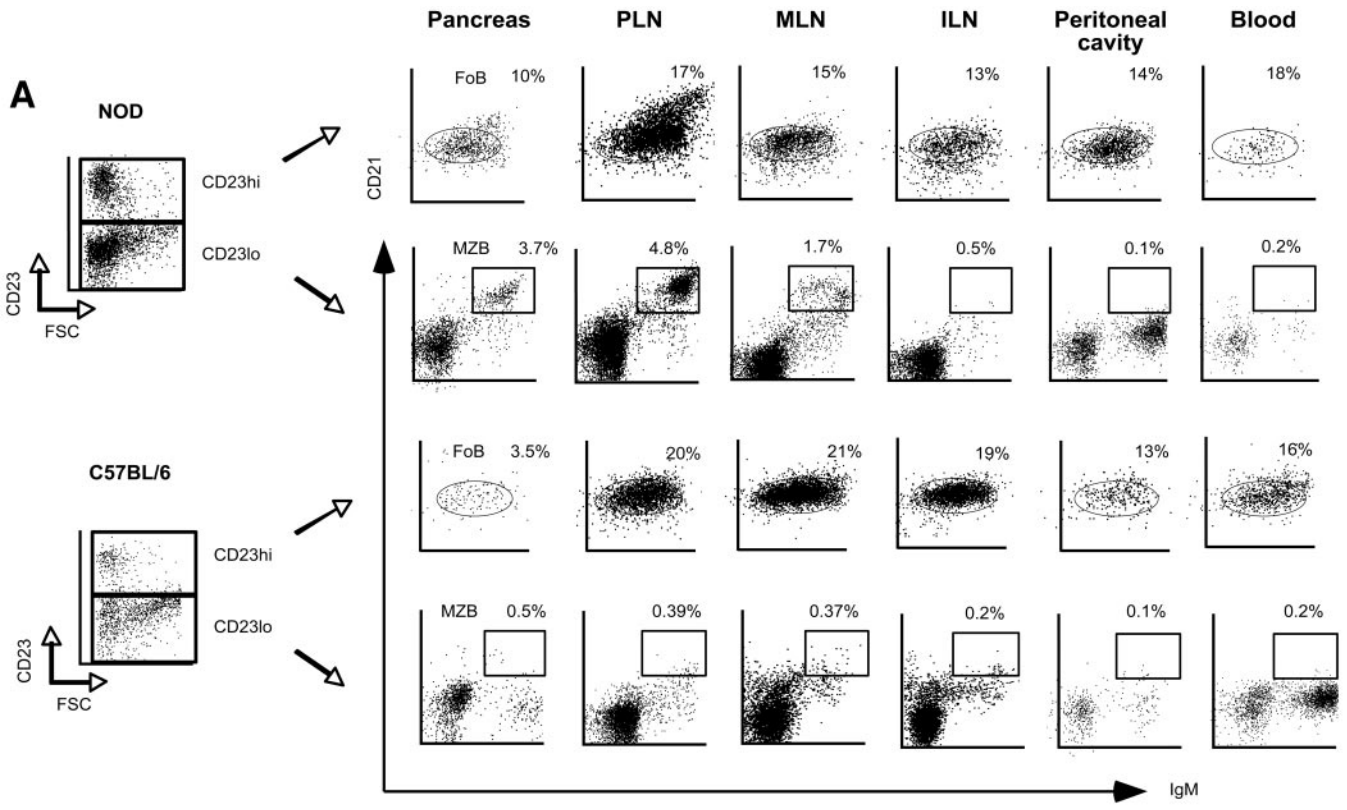

FIG. 6. MZBs colonize extrasplenic locations in female NOD mice. Representative FACS plots illustrating MZB colonization of pancreas, PLNs, MLNs, ILNs, peritoneal cavity, and peripheral blood of 16-week-old female NOD and C57BL/6 mice. Numbers indicate frequency of B subpopulation present as a percentage of total lymphocytes. Results are from one of at least six independent experiments with identical results.

fourfold ($n \geq 6$) ($P < 0.001$), from $\sim 2 \times 10^6$ to $\sim 8.3 \times 10^6$ at 12 weeks of age (Fig. 2*E*). Therefore, we show that MZB numbers do not remain static in NOD mice but show an age-dependent increase. Interestingly, this expansion correlates with the onset of frank diabetes in female NOD mice.

Altered S1P signaling in NOD mice. The increased accumulation of MZBs in the spleen of female NOD mice was clearly apparent by histological analysis, evidenced as an enlarged region of CD1d-bright cells colocalizing with MOMA-1^+ macrophages surrounding the follicles (Fig. 3*A*). MZB localization at the splenic marginal sinus is controlled by chemotactic cues provided by the lysophospholipid S1P and integrin-dependent interactions (27,29). Since expression of $\alpha 1\beta 2$ and $\beta 2$ integrins have been shown to be normal in NOD MZBs (10), we focused on examining the S1P pathway. We found that S1P1 and S1P3, the S1P receptors responsible for MZB retention (27), were significantly ($n = 3$) ($P < 0.001$) increased on MZBs from NOD versus C57BL/6 mice (Fig. 3*B*). Examination of the chemotactic response of MZBs to S1P revealed that NOD MZBs were approximately twofold more sensitive than MZBs from C57BL/6 mice to S1P at 1 nmol/l ($n = 3$) ($P < 0.001$) and 10 nmol/l ($n = 3$) ($P < 0.01$) (Fig. 3*C*). Pretreatment of NOD mice with FTY720 before harvesting the B-cells, to downregulate S1P1 expression (27), did not negatively impact the heightened response to S1P, suggesting that MZB chemotaxis was independent of S1P1, as has been previously reported (27). In contrast, NOD FoBs expressed normal levels of S1P1 and S1P3 (Fig. 3*B*) and, as expected (28), were not responsive to S1P (Fig. 3*D*). Together, these data indicate that NOD MZBs are hyperresponsive to chemotactic cues provided by S1P, due to an increase in S1P3 expression. The increased sensitivity of NOD MZBs to S1P may support their unusually magnified accumulation at the splenic marginal sinus.

Functional characteristics of NOD MZBs. We next examined MZB responses from NOD mice to mitogens and costimulatory ligands to determine whether their heightened chemotactic responses reflected a generalized hyperresponsiveness or was selective for particular pathways. MZB and FoB populations were isolated to 90% purity by a FACSorter, as depicted in Fig. 4*A*. As reported previously (16), we found that MZBs from either NOD or C57BL/6 mice responded poorly to B-cell receptor cross-linking (i.e., ≤500 cpm) (Fig. 4*B*), a phenotype ascribed to an increased sensitivity of MZBs to activation-induced apoptosis following B-cell receptor stimulation (16,17). However, we found that NOD MZBs were approximately twofold ($P < 0.001$, $n = 5$) more responsive to CD40 ligation than MZBs from C57BL/6 mice, a pattern that was heightened with the addition of interleukin-4 (Fig. 4*C* and *D*). That is, NOD MZBs were approximately fourfold ($n = 5$) ($P < 0.0001$) more responsive to CD40 plus interleukin-4 stimulation than MZBs from C57BL/6 mice. Moreover, NOD MZBs were ~10-fold ($n = 5$) ($P < 0.001$) more responsive to toll-like receptor (TLR) 9 stimulation than MZBs from C57BL/6 mice (Fig. 4*E*). In contrast, NOD and C57BL/6 MZBs were equally responsive to TLR4 stimulation (Fig. 4*F*).

We found that NOD FoBs proliferated strongly to B-cell receptor stimulation, as did FoBs from C57BL/6 mice (Fig. 4*B*). Similar to NOD MZBs, NOD FoBs were hyperresponsive to CD40 ligation in the presence, or absence, of interleukin-4, showing an approximately two- and three-

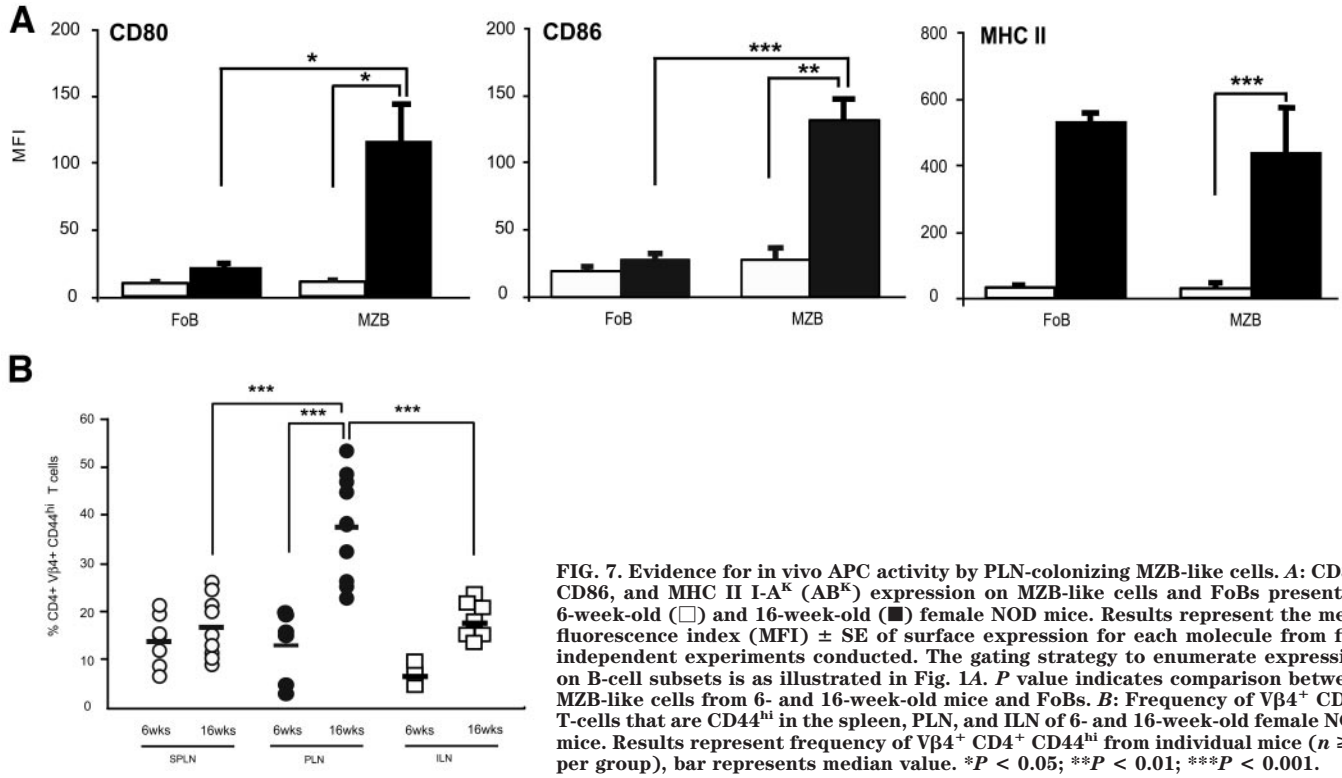

FIG. 7. Evidence for in vivo APC activity by PLN-colonizing MZB-like cells. *A*: CD80, CD86, and MHC II I-A^{K} (AB^{K}) expression on MZB-like cells and FoBs present in 6-week-old (□) and 16-week-old (■) female NOD mice. Results represent the mean fluorescence index (MFI) ± SE of surface expression for each molecule from five independent experiments conducted. The gating strategy to enumerate expression on B-cell subsets is as illustrated in Fig. 1*A*. *P* value indicates comparison between MZB-like cells from 6- and 16-week-old mice and FoBs. *B*: Frequency of Vβ4^{+} CD4^{+} T-cells that are CD44^{hi} in the spleen, PLN, and ILN of 6- and 16-week-old female NOD mice. Results represent frequency of Vβ4^{+} CD4^{+} CD44^{hi} from individual mice ($n \geq 6$ per group), bar represents median value. *$P < 0.05$; **$P < 0.01$; ***$P < 0.001$.

fold ($n = 5$) ($P < 0.01$) increase over the proliferative response of C57BL/6 FoBs, respectively (Fig. 4*C* and *D*). In contrast to MZBs, NOD and C57BL/6 FoBs showed equivalent proliferative responses to TLR9 and TLR4 stimulation (Fig. 4*E–F*). Thus, NOD FoBs do not exhibit the same pattern of hyperresponsiveness toward TLR9 stimulation as NOD MZBs. Therefore, NOD MZBs exhibit a cell-intrinsic pattern of hyperresponsiveness to selected B-cell mitogens, namely TLR9 ligation and CD40 ligation compared with MZBs from C57BL/6 mice.

NOD MZBs can present autoantigen to diabetogenic T-cells. One potential mechanism by which B-cells contribute to diabetes pathogenesis is as APCs, presenting autoantigens to self-reactive T-cells (5–7). We were curious as to whether MZBs were able to act as APCs, given that they were hyperresponsive to TLR ligation and CD40 ligation, stimuli important for the maturation and activation of dendritic cells (30,31). Unfractionated splenic NOD B-cells were able to present the insulin peptide B9:23 and efficiently drive T-cell proliferation ($n = 5$) ($P < 0.001$) (Fig. 5*A*). To examine the APC capacity of B-cell subsets, MZBs and FoBs were purified as in Fig. 4*A*. We found that MZBs were able to efficiently present the B9:23 peptide to self-reactive T-cells and elicit their proliferation ($n = 5$) ($P < 0.001$) (Fig. 5*B*). Indeed, MZBs could present B9:23 with similar efficiency ($n = 5$) ($P < 0.01$) to that of FoBs (Fig. 5*B* and *C*).

Having shown that MZBs could present insulin peptides to self-reactive T-cells, we next examined whether MZBs were able to capture and process intact insulin as an autoantigen. As has been shown previously (32), for both NOD and C57BL/6 B-cells, we also found that unfractionated B-cells could process and present insulin to diabetogenic T-cells (Fig. 5*D*). Significantly, we found that both MZBs ($n = 5$) ($P < 0.01$) and FoBs ($n = 5$) ($P < 0.05$) were able to effectively activate self-reactive T-cells (Fig. 5*E* and *F*), indicating that MZBs in particular are capable of capturing and processing intact autoantigens so as to present them as peptide–major histocompatibilty complex (MHC) complexes to self-reactive T-cells. Neither the MZB nor FoB populations alone were able to recapitulate the efficacy of unfractionated splenic B-cells as APC (Fig. 5*A–F*), suggesting that both subpopulations contribute to the APC activity of unfractionated B-cells.

NOD MZBs colonize the PLN and pancreas. The PLN is a critical site for the presentation of diabetes autoantigens to self-reactive T-cells (33–35). Since we demonstrated that splenic NOD MZBs can capture and present autoantigen to self-reactive T-cells, it was important that we examined whether MZBs were present in PLNs of NOD mice. A precedent for extrasplenic migration of MZBs has been seen in patients with Sjogren's syndrome and also BAFF transgenic and NZB/W F1 mice (22). We could detect an increased frequency of CD23^{low}, IgM^{hi}, and CD21^{hi} cells, a phenotype reminiscent of splenic MZBs, in the PLN of 16-week-old NOD mice (Fig. 6 vs. Fig. 1*A*). These MZB-like cells were not detected at the same frequency in the inguinal lymph node (ILN), mesenteric lymph node (MLN), the peripheral blood, or the peritoneal cavity of either NOD or C57BL/6 mice. These MZB-like cells were further characterized as being CD1d^{hi} and CD9^{hi} (data not shown), additional markers delineating MZBs in the spleen (36,37).

NOD B-cells present autoantigen to diabetogenic CD4^{+} T-cells (5–7), and we demonstrated that NOD MZBs exhibit APC activity. Significantly, we found that the MZB-like cells present in the PLNs were enriched for the expression of MHC class II, CD80, and CD86 at 16 vs. 6 weeks of age (Fig. 7*A*). Concordantly, the frequency of antigen-activated diabetogenic Vβ4^{+} CD4^{+} T-cells in the PLNs, as evidenced by high CD44 expression, was increased from ~12.75% in 6-week-old NOD mice to ~37.5% in 16-week-old NOD mice ($n = 5$) ($P < 0.001$) (Fig. 7*B*). Thus, the accumulation of MZB-like cells in the PLNs with

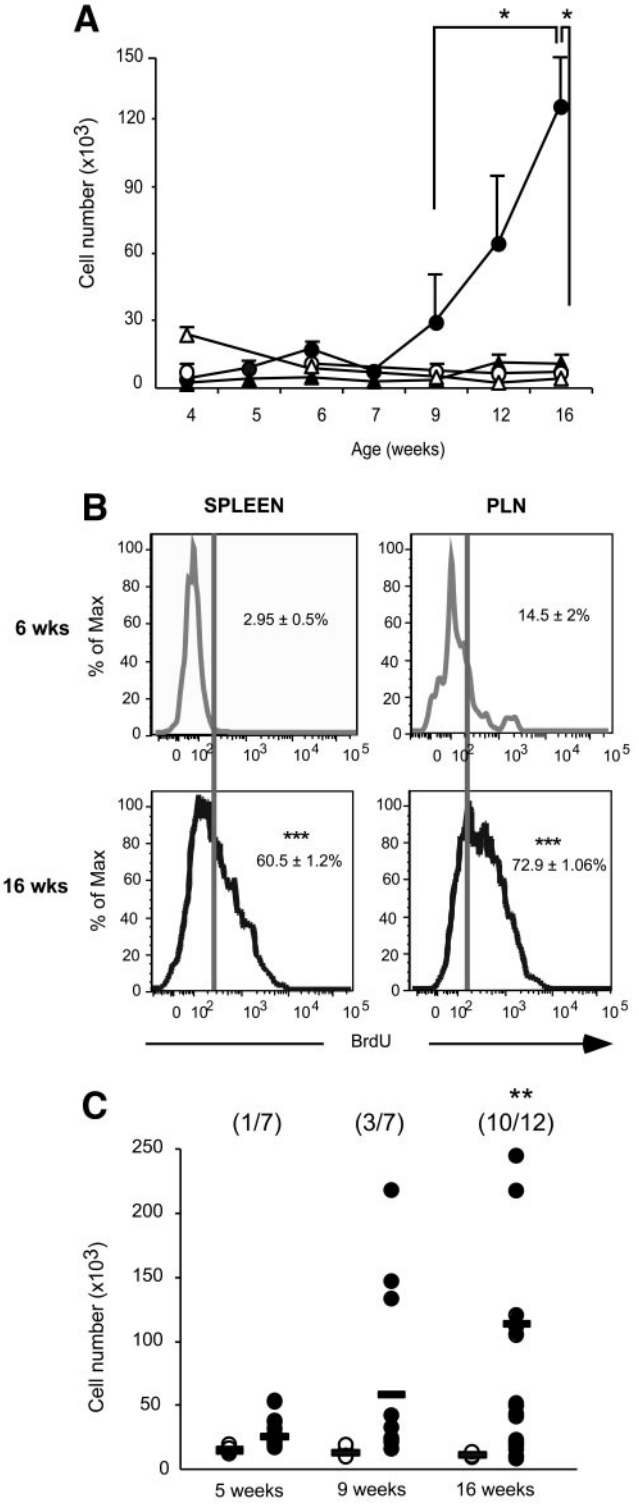

FIG. 8. Age-dependent accumulation of MZB-like cells in the PLN of female NOD mice. *A*: Calculated absolute MZB-like cell numbers in the PLN and ILN of female NOD and C57BL/6 mice was assessed over time ($n \geq 6$ mice examined at each time point). NOD PLN (●) and C57BL/6 PLN (○) and NOD ILN (▲) and C57BL/6 ILN (△). The gating strategy to enumerate splenic B-cell subsets is as illustrated in Fig. 1*A*. *P* values represent comparison between NOD PLN and age-matched control strain or comparison between different ages in NOD mice. *B*: Representative histograms showing BrdU incorporation in MZBs from spleen and PLN in 6- and 16-week-old female NOD mice after 3 days of in vivo BrdU labeling. MZB-like cells were identified as in Fig. 1*A*. *P* value indicates comparison between proliferation rates at 6 and 16 weeks of age. *C*: Calculated absolute numbers of MZB-like cells infiltrating the PLN of NOD (solid symbols) or C57BL/6 (open symbols) mice at the indicated ages. Results represent values from individual mice ($n \geq 5$ per group), bar represents median value. Number in parentheses indicates frequency of NOD mice with a MZB-like cell infiltrate age-matched C57BL/6 controls. *P* value relates number of MZB-like cells in NOD mice compared with age-matched C57BL/6 mice. *$P < 0.05$; **$P < 0.01$; ***$P < 0.001$.

a phenotype indicative of APC activity correlates with an increase in the frequency of antigen-experienced diabetogenic $CD4^+$ T-cells. Together with our in vitro studies (Fig. 5), these data support the concept that MZBs may be capable of presenting autoantigen in vivo.

Intriguingly, a $CD23^{low}$, but IgM^{hi}, $CD21^{hi}$ MZB-like population was also observed in the pancreas of NOD but not C57BL/6 mice (Fig. 6 vs. Fig. 1*A*). Using a cutoff of 1% determined from analysis of pancreata from C57BL/6 mice, we found that ~60% ($n = 31$ of 48) ($P < 0.001$) of female NOD mice between 4 and 16 weeks of age exhibited MZBs in the pancreas (MZB mean percentage ± SE = 3.89 ± 0.58%; $n = 31$). The increased number of MZB-like cells in the PLNs of NOD mice, and their localization to the pancreas, suggests that this does not represent random migration but rather was related to the pathophysiology of diabetes.

Age-dependent accumulation of MZB-like cells in the PLN. A longitudinal study to enumerate MZB-like cell numbers in the PLN over time revealed a marked ~15-fold increase ($n \geq 6$) ($P < 0.005$) in the absolute numbers of MZBs in NOD, but not C57BL/6 mice, at ~16 weeks of age (Fig. 8*A*). In contrast, neither the frequency nor number of MZBs in the ILN and MLN of NOD mice changed over this same period (Fig. 6 and Fig. 8*A*). To determine whether the increase in MZB-like cells in the PLN related to migration or proliferation locally, we analyzed MZB-like cell BrdU incorporation rates at 6 and 16 weeks of age. As shown in Fig. 8*B*, a substantial increase in the proliferation rates for MZBs of the spleen and MZB-like cells of the PLN was observed at 16 vs. 6 weeks of age in female NOD mice ($n \geq 5$ per group) ($P < 0.001$), correlating with the increase in absolute numbers of MZB-like cells in the PLN (Fig. 8*A*). Thus, local proliferation of MZB-like cells in the PLN contributes to their expansion at 16 weeks of age.

Using the numbers of MZBs in the PLN of age-matched C57BL/6 mice as a cutoff, it could be seen that the frequency of NOD mice with a number of MZB-like cells in the PLN greater than that observed for C57BL/6 also increased with age, reaching ~80% ($n > 7$) ($P < 0.01$) at 16 weeks of age (Fig. 8*C*). Of further interest is the similarity between the frequency of NOD mice harboring MZB-like cells in the PLN at 16 weeks of age and the incidence of type 1 diabetes in NOD mice.

DISCUSSION

One important role for B-cells in the pathogenesis of type 1 diabetes is as an APC (1), capturing and presenting autoantigen to self-reactive $CD4^+$ T-cells driving their activation and expansion (5–7). To date, the role of MZBs versus FoBs as APCs has not been considered in this context. Here, we here provide the first evidence that in the NOD model of diabetes, MZB have the potential to break tolerance to autoantigens by virtue of their capacity to present insulin-derived peptide-MHCs to self-reactive T-cells. We found that MZBs were neither the only B-cell subtype with this function, nor the most efficacious, at least in vitro, where MZBs and FoBs exhibit a similar capacity to activate diabetogenic T-cells. However, the

contribution of different B-cell subsets as important APCs in vivo will be determined by their relative ratios at specific anatomical locations and also by their activation status.

In this regard, the extrasplenic localization of MZB-like cells may be particularly significant. The expansion and aberrant migration of MZBs is associated with autoimmunity in BAFF transgenic mice (20), which develop pathologies reminiscent of Sjogren's syndrome and systemic lupus eyrthematosus (22). In BAFF transgenic mice, MZBs migrate to disease-related sites, including lymph nodes but also the salivary gland, the target organ in Sjogren's syndrome (38). In human subjects with Sjogren's syndrome, $CD27^+$ memory B-cells, analogous to rodent MZBs, are present in the peripheral blood and colonize the salivary glands (38). With respect to diabetes pathogenesis, the PLN is recognized as a site critical for the presentation of autoantigen to self-reactive T-cells (33–35). We show that MZB-like cells accumulate at this site in increasing numbers in an age-dependent manner, suggesting that is not a random event but rather is closely linked to the conversion to overt diabetes in the NOD model.

Regarding the activation status of NOD MZBs, we demonstrate that NOD MZBs exhibit a selective hyperresponsiveness to S1P, TLR9, and CD40 ligation as well as enhanced expression of costimulatory molecules. The molecular cause for some of these changes may relate to enhanced nuclear factor (NF)-κB signaling. NOD B-cells exhibit an exaggerated basal level of NF-κB activation (32), which may sensitize them to NF-κB–responsive signaling pathways such as CD40 and TLR9 to increase S1P receptor CD80 and CD86 expression. Of note, BAFF activates NF-κB (22), and B-cells from autoimmune-prone BAFF transgenic mice also accumulate at the marginal sinus (20) and are enriched for APC activity (39), which is supportive of a link between activation of NF-κB and B-cell APC function in autoimmunity.

Signals received through TLRs and CD40 are important for the maturation of professional APCs such as dendritic cells, favoring their acquisition of a phenotype that supports the induction of antigen-specific T-cell–dependent immunity (30,31,40). We demonstrate that NOD MZBs can process and present autoantigen. The MZB-like cells of the PLN exhibit a number of features indicative of in vivo activation and enhanced APC potential. This includes their increased proliferative status, a classic hallmark of lymphocyte activation, and also their high expression levels of costimulatory molecules. Significantly, the presence of these activated MZB-like cells correlated with an increased frequency of activated diabetogenic $CD4^+$ T-cells in the PLN, consistent with their demonstrated APC potential.

The natural ability of MZBs to rapidly respond to innate signals (24), as well as present antigen to T-cells (18), conceptually places MZBs within a unique position in the immune system as cells being able to connect innate with adaptive immune responses. This may have relevance for the etiology of type 1 diabetes because though an innate trigger for diabetes has not been convincingly shown, it is highly speculated that such an event precipitates the activation of self-reactive T-cells and subsequent β-cell destruction (41,42). The specialized role of MZBs in immunity, coupled with the altered features of the NOD MZB compartment we now present, marks MZBs as candidate players in the series of events leading toward autoimmunity. We argue that MZBs may be important in diabetes pathogenesis by virtue of their capacity to respond to, and thus integrate, innate-derived inflammatory signals with the capture and presentation of autoantigens, enabling MZBs to direct effector T-cell responses against β-cell autoantigens.

ACKNOWLEDGMENTS

E.M. is supported by a National Health and Medical Research Council Dora Lush Fellowship. This work has been supported by grant 5-2005-1132 from the Juvenile Diabetes Research Federation and a New South Wales BioFirst Award (to S.T.G.).

We would like to thank Dr. Pablo Silveira for helpful comments and critical reading of this manuscript. We also gratefully acknowledge the expert technical assistance of Michael Pickering and Eric Schmied.

REFERENCES

1. Silveira PA, Grey ST: B-cells in the spotlight: innocent bystanders or major players in the pathogenesis of type 1 diabetes. *Trends Endocrinol Metab* 17:128–135, 2006
2. Noorchashm H, Noorchashm N, Kern J, Rostami SY, Barker CF, Naji A: B-cells are required for the initiation of insulitis and sialitis in nonobese diabetic mice. *Diabetes* 46:941–946, 1997
3. Serreze DV, Chapman HD, Varnum DS, Hanson MS, Reifsnyder PC, Richard SD, Fleming SA, Leiter EH, Shultz LD: B lymphocytes are essential for the initiation of T cell-mediated autoimmune diabetes: analysis of a new "speed congenic" stock of NOD.Ig mu null mice. *J Exp Med* 184:2049–2053, 1996
4. Greeley SA, Katsumata M, Yu L, Eisenbarth GS, Moore DJ, Goodarzi H, Barker CF, Naji A, Noorchashm H: Elimination of maternally transmitted autoantibodies prevents diabetes in nonobese diabetic mice. *Nat Med* 8:399–402, 2002
5. Noorchashm H, Lieu YK, Noorchashm N, Rostami SY, Greeley SA, Schlachterman A, Song HK, Noto LE, Jevnikar AM, Barker CF, Naji A: I-Ag7-mediated antigen presentation by B lymphocytes is critical in overcoming a checkpoint in T cell tolerance to islet beta cells of nonobese diabetic mice. *J Immunol* 163:743–750, 1999
6. Serreze DV, Fleming SA, Chapman HD, Richard SD, Leiter EH, Tisch RM: B lymphocytes are critical antigen-presenting cells for the initiation of T cell-mediated autoimmune diabetes in nonobese diabetic mice. *J Immunol* 161:3912–3918, 1998
7. Falcone M, Lee J, Patstone G, Yeung B, Sarvetnick N: B lymphocytes are crucial antigen-presenting cells in the pathogenic autoimmune response to GAD65 antigen in nonobese diabetic mice. *J Immunol* 161:1163–1168, 1998
8. Loder F, Mutschler B, Ray RJ, Paige CJ, Sideras P, Torres R, Lamers MC, Carsetti R: B-cell development in the spleen takes place in discrete steps and is determined by the quality of B-cell receptor-derived signals. *J Exp Med* 190:75–89, 1999
9. Martin F, Kearney JF: B-cell subsets and the mature preimmune repertoire. Marginal zone and B1 B-cells as part of a "natural immune memory." *Immunol Rev* 175:70–79, 2000
10. Rolf J, Motta V, Duarte N, Lundholm M, Berntman E, Bergman ML, Sorokin L, Cardell SL, Holmberg D: The enlarged population of marginal zone/CD1d(high) B lymphocytes in nonobese diabetic mice maps to diabetes susceptibility region Idd11. *J Immunol* 174:4821–4827, 2005
11. Quinn WJ 3rd, Noorchashm N, Crowley JE, Reed AJ, Noorchashm H, Naji A, Cancro MP: Cutting edge: impaired transitional B-cell production and selection in the nonobese diabetic mouse. *J Immunol* 176:7159–7164, 2006
12. Noorchashm H, Moore DJ, Lieu YK, Noorchashm N, Schlachterman A, Song HK, Barker CF, Naji A: Contribution of the innate immune system to autoimmune diabetes: a role for the CR1/CR2 complement receptors. *Cell Immunol* 195:75–79, 1999
13. Pillai S, Cariappa A, Moran ST: Marginal zone B-cells. *Annu Rev Immunol* 23:161–196, 2005
14. Song H, Cerny J: Functional heterogeneity of marginal zone B-cells revealed by their ability to generate both early antibody-forming cells and germinal centers with hypermutation and memory in response to a T-dependent antigen. *J Exp Med* 198:1923–1935, 2003
15. Snapper CM, Yamada H, Smoot D, Sneed R, Lees A, Mond JJ: Comparative in vitro analysis of proliferation, Ig secretion, and Ig class switching by murine marginal zone and follicular B-cells. *J Immunol* 150:2737–2745, 1993

16. Oliver AM, Martin F, Kearney JF: IgMhighCD21high lymphocytes enriched in the splenic marginal zone generate effector cells more rapidly than the bulk of follicular B-cells. *J Immunol* 162:7198–7207, 1999
17. Oliver AM, Martin F, Gartland GL, Carter RH, Kearney JF: Marginal zone B-cells exhibit unique activation, proliferative and immunoglobulin secretory responses. *Eur J Immunol* 27:2366–2374, 1997
18. Attanavanich K, Kearney JF: Marginal zone, but not follicular B-cells, are potent activators of naive CD4 T cells. *J Immunol* 172:803–811, 2004
19. Martin F, Oliver AM, Kearney JF: Marginal zone and B1 B-cells unite in the early response against T-independent blood-borne particulate antigens. *Immunity* 14:617–629, 2001
20. Batten M, Groom J, Cachero TG, Qian F, Schneider P, Tschopp J, Browning JL, Mackay F: BAFF mediates survival of peripheral immature B lymphocytes. *J Exp Med* 192:1453–1466, 2000
21. Wellmann U, Werner A, Winkler TH: Altered selection processes of B lymphocytes in autoimmune NZB/W mice, despite intact central tolerance against DNA. *Eur J Immunol* 31:2800–2810, 2001
22. Mackay F, Sierro F, Grey ST, Gordon TP: The BAFF/APRIL system: an important player in systemic rheumatic diseases. *Curr Dir Autoimmun* 8:243–265, 2005
23. Theofilopoulos AN, Dixon FJ: Murine models of systemic lupus erythematosus. *Adv Immunol* 37:269–390, 1985
24. Martin F, Kearney JF: Marginal-zone B-cells. *Nat Rev Immunol* 2:323–335, 2002
25. Grey ST, Longo C, Shukri T, Patel VI, Csizmadia E, Daniel S, Arvelo MB, Tchipashvili V, Ferran C: Genetic engineering of a suboptimal islet graft with A20 preserves beta cell mass and function. *J Immunol* 170:6250–6256, 2003
26. Liuwantara D, Elliot M, Smith MW, Yam AO, Walters SN, Marino E, McShea A, Grey ST: Nuclear factor-κB regulates β-cell death: a critical role for A20 in β-cell protection. *Diabetes* 55:2491–2501, 2006
27. Cinamon G, Matloubian M, Lesneski MJ, Xu Y, Low C, Lu T, Proia RL, Cyster JG: Sphingosine 1-phosphate receptor 1 promotes B-cell localization in the splenic marginal zone. *Nat Immunol* 5:713–720, 2004
28. King C, Ilic A, Koelsch K, Sarvetnick N: Homeostatic expansion of T cells during immune insufficiency generates autoimmunity. *Cell* 117:265–277, 2004
29. Lu TT, Cyster JG: Integrin-mediated long-term B-cell retention in the splenic marginal zone. *Science* 297:409–412, 2002
30. Serra P, Amrani A, Yamanouchi J, Han B, Thiessen S, Utsugi T, Verdaguer J, Santamaria P: CD40 ligation releases immature dendritic cells from the control of regulatory CD4+CD25+ T cells. *Immunity* 19:877–889, 2003
31. Pasare C, Medzhitov R: Toll-dependent control mechanisms of CD4 T cell activation. *Immunity* 21:733–741, 2004
32. Wheat W, Kupfer R, Gutches DG, Rayat GR, Beilke J, Scheinman RI, Wegmann DR: Increased NF-kappa B activity in B-cells and bone marrow-derived dendritic cells from NOD mice. *Eur J Immunol* 34:1395–1404, 2004
33. Jaakkola I, Jalkanen S, Hanninen A: Diabetogenic T cells are primed both in pancreatic and gut-associated lymph nodes in NOD mice. *Eur J Immunol* 33:3255–3264, 2003
34. Hoglund P, Mintern J, Waltzinger C, Heath W, Benoist C, Mathis D: Initiation of autoimmune diabetes by developmentally regulated presentation of islet cell antigens in the pancreatic lymph nodes. *J Exp Med* 189:331–339, 1999
35. Gagnerault MC, Luan JJ, Lotton C, Lepault F: Pancreatic lymph nodes are required for priming of beta cell reactive T cells in NOD mice. *J Exp Med* 196:369–377, 2002
36. Amano M, Baumgarth N, Dick MD, Brossay L, Kronenberg M, Herzenberg LA, Strober S: CD1 expression defines subsets of follicular and marginal zone B-cells in the spleen: beta 2-microglobulin-dependent and independent forms. *J Immunol* 161:1710–1717, 1998
37. Won WJ, Kearney JF: CD9 is a unique marker for marginal zone B-cells, B1 cells, and plasma cells in mice. *J Immunol* 168:5605–5611, 2002
38. Groom JR, Fletcher CA, Walters SN, Grey ST, Watt SV, Sweet MJ, Smyth MJ, Mackay CR, Mackay F: BAFF and MyD88 signals promote a lupuslike disease independent of T cells. *J Exp Med* 204:1959–1971, 2007
39. Yang M, Hase H, Legarda-Addison D, Varughese L, Seed B, Ting AT: B-cell maturation antigen, the receptor for a proliferation-inducing ligand and B-cell-activating factor of the TNF family, induces antigen presentation in B-cells. *J Immunol* 175:2814–2824, 2005
40. Ridge JP, Di Rosa F, Matzinger P: A conditioned dendritic cell can be a temporal bridge between a CD4+ T-helper and a T-killer cell. *Nature* 393:474–478, 1998
41. Benoist C, Mathis D: Autoimmunity provoked by infection: how good is the case for T cell epitope mimicry? *Nat Immunol* 2:797–801, 2001
42. Karin M, Lawrence T, Nizet V: Innate immunity gone awry: linking microbial infections to chronic inflammation and cancer. *Cell* 124:823–835, 2006